


 Cite this: *Chem. Commun.*, 2024, 60, 11359

 Received 21st August 2024,
 Accepted 10th September 2024

DOI: 10.1039/d4cc04266b

rsc.li/chemcomm

Hypervalent zinc(i) complexes with an NNNN-macrocycle: C–H bond activation across the zinc(i)–zinc(i) bond†

 Pritam Mahawar,^a Thayalan Rajeshkumar,^b Thomas P. Spaniol,^a Laurent Maron^{id}^b and Jun Okuda^{id}^{*a}

Hetero- and homoleptic dinuclear zinc(i) complexes containing the macrocycle Me₄TACD (*N,N',N'',N'''*-1,4,7,10-tetramethylcyclododecane) were prepared; the heteroleptic complex [(Me₄TACD)Zn–ZnCp*]⁺ reacted with activated hydrocarbons R–H (R = CH₂CN, C≡CPh) to give the corresponding hydrocarbonyl zinc(ii) complexes [(Me₄TACD)ZnR]⁺.

The discovery of decamethylzincocene Cp*Zn–ZnCp* (Cp* = η⁵-C₅Me₅) by Carmona *et al.* in 2004¹ has prompted the isolation of other complexes featuring the remarkable zinc(i)–zinc(i) σ-bond. On the one hand, neutral zinc(i) analogs containing a L₂X-type ligand (L = two-electron, X = one-electron ligand)^{2a} such as bulky aryl (l = 0)³ and β-diketiminato (l = 1)⁴ became known, on the other hand protonolysis or oxidation of Cp*Zn–ZnCp* allowed the synthesis of mono(cations) of the type [(L₃)Zn–ZnCp*]⁺ (ref. 5) or dicationic complexes [(L₃)Zn–Zn(L₃)]²⁺ (L = THF, DMAP).⁶ Regarding zinc as a main group element with filled 3d¹⁰ shell,^{2b} the valence electron count of zinc in all these complexes does not exceed 8 electrons.^{2,7} Recently, we have reported that the heteroleptic zinc(i) cation [(TEEDA)(thf)Zn–ZnCp*]⁺[BAR₄^F][−] (TEEDA = *N,N,N',N'*-tetraethylethylenediamine; Ar^F = 3,5-((CF₃)₂C₆H₃)) can undergo a heterolytic dihydrogen cleavage.⁸ As recently suggested for the reactivity of diberyllocene,⁹ main group metal–metal bonds can be polarized, so for decamethylzincocene a resonance structure [Cp*Zn(i)]⁺ ← [Zn(0)Cp*][−] can be implied, accounting for some of the reactivity patterns (redox disproportionation) observed.¹⁰ We wondered whether introducing hypervalency⁷ at the zinc(i) center (with

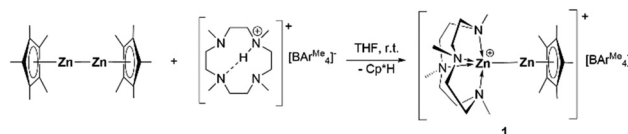
formal valence electron count higher than 8) would result in a higher reactivity of the zinc(i)–zinc(i) bond. Here we report on the preparation of both homo- and heteroleptic zinc(i) cations that contain the L₄-type macrocycle Me₄TACD (*N,N',N'',N'''*-1,4,7,10-tetramethylcyclododecane).¹¹ The heteroleptic zinc(i) cation was found to undergo a heterolytic C–H bond activation of acetonitrile and phenylacetylene.^{10,12}

The versatile macrocyclic ligand Me₄TACD is capable of coordinating s-,¹³ and p-block¹⁴ metal cations including low-valent triel cations Ga(i), In(i) and Tl(i). Thus, stoichiometric reaction of Cp*Zn–ZnCp* with the borate salt of the protonated Me₄TACD [(Me₄TACD)H][BAR₄^{Me}]¹⁵ (BAR₄^{Me} = [B{3,5-(CH₃)₂-C₆H₃]₄)[−] in THF at room temperature for one hour afforded the heteroleptic zinc(i) monocation [(Me₄TACD)Zn–ZnCp*][BAR₄^{Me}] (**1**) in 90% yield with the elimination of one equivalent of Cp*H. Colorless compound **1** is stable under argon at room temperature and is soluble in THF, acetonitrile, and dichloromethane (Scheme 1).

Compound **1** was characterized in solution using multinuclear NMR spectroscopy, including ¹H, ¹³C, and ¹¹B, and in the solid state using single crystal X-ray diffraction. The ¹H NMR spectra indicate η⁵-Cp* coordination, displaying a characteristic single peak for all methyl groups of Cp* at δ 2.02 ppm and confirmed the ligand/borate ratio of 1:1. The diastereotopic CH₂CH₂ protons of the Me₄TACD ligand appear as multiplets of AA'BB' spin system in the range of δ 2.14–2.31 ppm, as commonly observed for the coordinated Me₄TACD ligand.¹⁴ The ¹³C{¹H} NMR spectrum revealed two signals for the Cp* methyl and ring carbons at δ 10.5 and δ 108.4 ppm, respectively, along with the peaks for the Me₄TACD ligand and

^a Institute of Inorganic Chemistry, RWTH Aachen University, Landoltweg 1, 52056 Aachen, Germany. E-mail: jun.okuda@ac.rwth-aachen.de

^b CNRS, INSA, UPS, UMR 5215, LPCNO, Université de Toulouse, 135 Avenue de Rangueil, 31077 Toulouse, France. E-mail: laurent.maron@irsamc.ups-tlse.fr

 † Electronic supplementary information (ESI) available: Experimental, analytical (NMR, IR spectra, elemental analysis) and crystallographic data of **1–4**. CCDC 2378377 (**1**), 2378378 (**2**), 2378379 (**3**) and 2378380 (**4**). For ESI and crystallographic data in CIF or other electronic format see DOI: <https://doi.org/10.1039/d4cc04266b>

 Scheme 1 Synthesis of [(Me₄TACD)Zn–ZnCp*][BAR₄^{Me}] (**1**).

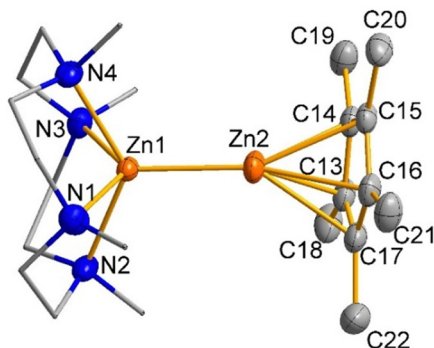
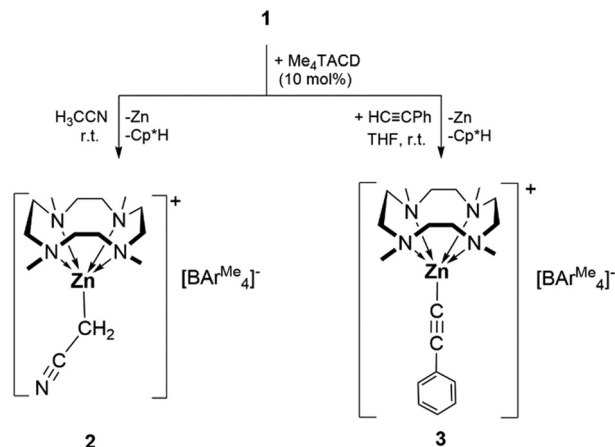



Fig. 1 Cationic part of the molecular structure of compound **1**. Selected interatomic distances [Å] and angles [°]: Zn1–Zn2 2.3510(3), Zn1–N1 2.2388(17), Zn1–N2 2.2177(15), Zn1–N3 2.2550(15), Zn1–N4 2.2181(15), Zn1–C13 2.3484(18), Zn1–C14 2.3168(18), Zn1–C15 2.2779(17), Zn1–C16 2.2889(18), Zn1–C17 2.3275(18), N1–Zn1–N2 80.40(6), N1–Zn1–N3 130.33(6), N1–Zn1–N4 79.98(6), N1–Zn1–Zn2 115.79(4), N2–Zn1–Zn2 112.12(4), N3–Zn1–Zn2 113.83(4), N4–Zn1–Zn2 117.99(4).

borate counter-ion. Compound **1** crystallizes in the monoclinic space group $P2_1/n$ with one ion pair per asymmetric unit. The structure of the molecular cation is depicted in Fig. 1 (see ESI† for details). The cationic penta-coordinate zinc center is positioned above the N_4 -basal plane of the Me_4TACD ligand with the Zn– $N_{(centroid)}$ bond distance of 0.9416(6) Å, which is consistent with the Zn– $N_{(centroid)}$ bond distance (0.9371(15) Å) in the zinc(II) hydride cation $[(Me_4TACD)ZnH][HBPh_3]$.¹⁶ The zinc–zinc distance of 2.3510(3) Å is marginally longer than the reported value for heteroleptic Zn(I) monocations $[(Et_2O)_3Zn-ZnCp^*][BAR_4^F]$ (2.324(2) Å)⁵ and $[(TEEDA)Zn-ZnCp^*][BAR_4^F]$ (2.3253(15) Å).⁸ The enhanced polarization effect caused by the increased coordination number and asymmetrical ligand environment causes the zinc–zinc bond distance to be longer than in $Cp^*Zn-ZnCp^*$ with 2.302(1) Å.¹

Compound **1** shows a slight slipping of the Cp^* ring from η^5 -coordination to Zn1, with the metal atom's projection displaced from the ring's centroid by 0.072 Å. The Zn1– $Cp^*_{(centroid)}$ distance (1.971 Å) lies within the range of the Zn1– $Cp^*_{(centroid)}$ bond distances in heteroleptic zinc(I) complexes $[(TEEDA)Zn-ZnCp^*][BAR_4^F]$ (1.954 Å)⁸ and $[(HC\{C(Me)NDipp\}_2)Zn-ZnCp^*]$ (1.9215(3) Å).¹⁷ This slipped coordination results in the non-linear alignment of the Zn2–Zn1– $Cp^*_{(centroid)}$ bond angle of 164.75(1)° in **1**.

Reactivity studies of zinc(I) complexes toward activated hydrocarbons are scarce,¹⁰ although reactions with phenylacetylene have been studied.^{10a–c} While the zinc(I) cation **1** is kinetically robust in acetonitrile for at least 12 h, in the presence of 10 mol% of Me_4TACD , the formation of a grey precipitate was observed within 5 min and zinc(II) cyanomethanide $[(Me_4TACD)Zn(CH_2CN)][BAR_4^{Me}]$ (**2**) was isolated from the supernatant in 85% yield (Scheme 2). Formation of **2** can be interpreted as a product of oxidative C–H bond addition across the Zn–Zn bond of **1**, presumably also forming unstable $[Cp^*ZnH]$,¹⁸ which is known to decompose *via* reductive elimination to form the observed byproducts Cp^*H and metallic zinc. Compound **2** can also be synthesized in THF using 2

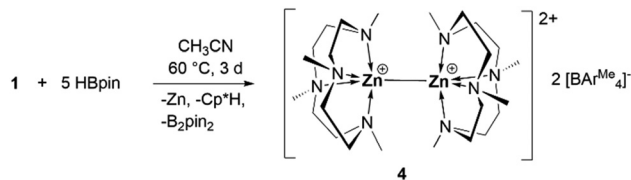


Scheme 2 Reaction of $[Me_4TACDZn-ZnCp^*][BAR_4^{Me}]$ (**1**) with activated hydrocarbons.

equivalents of acetonitrile in the presence of 10 mol% of Me_4TACD . Likewise, in the presence of 10 mol% of Me_4TACD , the reaction of compound **1** with phenylacetylene in THF at room temperature gave the zinc(II) acetylide complex $[(Me_4TACD)ZnC\equiv CPh][BAR_4^{Me}]$ (**3**) in 90% isolated yield (Scheme 2). The precise role of Me_4TACD is unclear, it may act as a Brønsted base in these reactions. Compounds **2** and **3** are soluble in THF, acetonitrile, and dichloromethane and are stable at room temperature under argon. Compounds **2** and **3** were characterized using multinuclear NMR spectroscopy (1H , ^{13}C , ^{11}B) in the solution state. The solid-state characterization was performed using single-crystal XRD and IR spectroscopy. In the 1H and $^{13}C\{^1H\}$ NMR spectra of compound **2** the characteristic peaks for the CH_2CN protons appear at δ 0.52 ppm and δ –14.3 ppm, respectively. For the acetylide compound **3** the $^{13}C\{^1H\}$ NMR spectrum shows the characteristic peaks for the acetylenic carbon atoms at δ 109.0 and 107.8 ppm. All peaks of the Me_4TACD ligands in compounds **2** and **3** are downfield shifted compared to those of **1**, due to the increase in oxidation number of zinc from +1 in compound **1** to +2 in compounds **2** and **3**.

Single crystal X-ray diffraction studies revealed the monomeric structure of compounds **2** and **3** (see ESI†). The coordination of the Me_4TACD ligand at the cationic zinc(II) center in compounds **2** and **3** is comparatively stronger than in precursor **1** with zinc(I) cation which can be seen by the decrease in the Zn– $N_{(centroid)}$ bond distance (0.8856(16) Å for **2** and 0.8776(9) Å for **3**) from 0.9416(6) (for **1**). The Zn– CH_2 bond distance in compound **2** of 2.025(3) Å is comparable to the Zn– CH_2 bond length in the pyrazolylborate- $[(Tp^{Ph,Me})Zn(CH_2CN)]$; $Tp^{Ph,Me}$ = hydrotris((5,3-methylphenyl-pyrazolyl)borate) 2.052(3) Å^{19a} and PMDTA-supported zinc cyanomethanide and (PMDTA = N,N,N',N',N' -pentamethyldiethylenetriamine, 1.991(6) Å) reported.^{19b} The $C\equiv C$ bond length in **3** (1.207(3) Å) is longer than that in free phenylacetylene (1.183(2) Å) due to the donation of π -electron to zinc vacant orbitals. The Zn–C bond length in compound **3** (1.9519(17) Å) lies within the range observed for the monomeric $[(dipp)NacNac]ZnC\equiv CPh$ (1.906(2) Å) ($(dipp)NacNac$ = 2-((2,6-diisopropyl-phenyl)amino)-4-((2,6-diisopropylphenyl)





Scheme 3 Formation of $[(\text{Me}_4\text{TACD})\text{Zn}-\text{Zn}(\text{Me}_4\text{TACD})][\text{BAR}_4^{\text{Me}}]_2$ (**4**).

imino}pent-2-enyl).²⁰ In the IR spectrum of compound **2** a stretching band at $\nu(\text{CN}) = 2193 \text{ cm}^{-1}$ indicates the presence of a terminal $\text{C}\equiv\text{N}$ group.

In analogy to the synthesis of **1** through protonation of one of the Cp^* ligands in $\text{Cp}^*\text{Zn}-\text{ZnCp}^*$, we attempted to protonate both Cp^* ligands by reacting with 2 equivalents of the acid $[(\text{Me}_4\text{TACD})\text{H}][\text{BAR}_4^{\text{Me}}]$. This only led to the formation of zinc(i) cation **1** along with unreacted acid. Recently, we reported that the zinc–zinc bond of zinc(i) cation $[(\text{TEEDA})\text{Zn}-\text{ZnCp}^*][\text{BAR}_4^{\text{F}}]$ can cleave dihydrogen in a heterolysis, similar to a frustrated Lewis acid–base type activation.⁸ When the reaction of compound **1** was carried out with a large excess (5 equivalents) of HBpin in acetonitrile at 60°C for 3 days, the zinc(i)–zinc(i) dication $[(\text{Me}_4\text{TACD})\text{Zn}-\text{Zn}(\text{Me}_4\text{TACD})][\text{BAR}_4^{\text{Me}}]_2$ (**4**) was formed along with Cp^*H , zinc metal, and B_2pin_2 (Scheme 3). Compound **4** was isolated in 30% yield (based on $(\text{Me}_4\text{TACD})\text{Zn}$) and characterized in the solution state using multinuclear NMR spectroscopy and in the solid state using single crystal XRD studies.

In the ^1H NMR spectrum of compound **4**, all the Me_4TACD protons (δ 2.33–2.51 ppm (CH_2) and δ 2.20 ppm (CH_3)) are deshielded compared to those in **1** (δ 2.14–2.31 ppm (CH_2) and δ 2.11 ppm (CH_3)) due to the increase in the cationic charge of the zinc centers. ^{13}C NMR spectra show all the corresponding signals for the Me_4TACD ligand and borate counterion. Compound **4** crystallizes in the orthorhombic space group $Pbca$ with one ion pair in the asymmetric unit. The dinuclear structure of **4** with a zinc(i)–zinc(i) distance of $2.4860(6) \text{ \AA}$ was confirmed using single crystal XRD diffraction (Fig. 2a). Due to the higher coordination number in **4**, the zinc–zinc bond distance is significantly longer than the zinc–zinc bond in the reported dications of the type $[\text{Zn}_2(\text{L}_6)]^{2+}$ $[\text{Zn}_2(\text{dmap})_6][\text{A}-\text{I}(\text{OC}(\text{CF}_3)_3)_4]_2$ ($2.419(2) \text{ \AA}$)^{6a} and $[\text{Zn}_2(\text{thf})_6][\text{BAR}_4^{\text{F}}]_2$ ($2.363(2) \text{ \AA}$).^{6b} As can be seen from the space-filling model (Fig. 2b), the two 9-electron $[\text{Zn}(\text{Me}_4\text{TACD})]^+$ units are closely meshed and the two Me_4TACD ligands adopt a staggered conformation (Fig. 2c). Notably, both ligands show $\delta\delta\delta\delta$ or $\lambda\lambda\lambda\lambda$ conformation of the CH_2CH_2 units and the overall molecular symmetry of the homochiral dimer corresponds to the rare pointgroup D_4 .

To provide further insight into the bonding in compounds **1** and **4**, DFT calculations were performed at the B3PW91 level of theory. Gas phase optimized structure agrees well with the experimentally determined structures of **1** and **4** from X-ray diffraction studies. The LUMO is mainly located on the Me_4TACD ligand in both compounds. The zinc–zinc bond in compound **1** constitutes the HOMO–2, while the HOMO is localized on $\text{Zn}-\text{Cp}^*$ bond. In contrast, the HOMO is mainly localized on the zinc–zinc bond in compound **4** (Fig. 3). This is consistent with the apparent longer zinc–zinc bond in

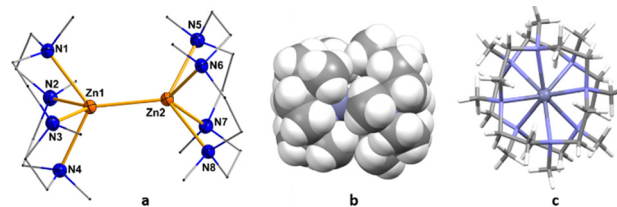


Fig. 2 (a) Left: Cationic part of the molecular structure of compound **4**. The anion part $[\text{BAR}_4^{\text{Me}}]$ and all H atoms are omitted for clarity. Displacement parameters are shown at 30% probability; selected interatomic distances [\AA] and angles [$^\circ$]: $\text{Zn1}-\text{N1}$ 2.378(3), $\text{Zn1}-\text{N2}$ 2.337(3), $\text{Zn1}-\text{N3}$ 2.390(3), $\text{Zn1}-\text{N4}$ 2.326(3), $\text{Zn1}-\text{Zn2}$ 2.4860(6), $\text{Zn2}-\text{N5}$ 2.480(3), $\text{Zn2}-\text{N6}$ 2.291(3), $\text{Zn2}-\text{N7}$ 2.463(3), $\text{Zn2}-\text{N8}$ 2.278(3); $\text{N1}-\text{Zn1}-\text{N2}$ 76.31(11), $\text{N1}-\text{Zn1}-\text{N3}$ 120.82(11), $\text{N1}-\text{Zn1}-\text{N4}$ 75.92(11), $\text{N1}-\text{Zn1}-\text{Zn2}$ 120.99(8), $\text{N2}-\text{Zn1}-\text{Zn2}$ 119.19(8), $\text{N3}-\text{Zn1}-\text{Zn2}$ 118.18(8), $\text{N4}-\text{Zn1}-\text{Zn2}$ 119.86(8). (b) Middle: Space filling model of **4**. (c) Right: View of **4** along the $\text{Zn}-\text{Zn}$ axis, highlighting the D_4 symmetry.

compound **4** ($2.4860(6) \text{ \AA}$) compared to **1** ($2.3510(3) \text{ \AA}$). Moreover, the presence of HOMO contribution in $\text{Zn}-\text{Cp}^*$ moiety goes in line with its reaction with the acidic proton of CH_3CN and $\text{HC}\equiv\text{CPh}$ for the formation of HZnCP^* .

The mechanism for the formation of **4** remains obscure. It seems plausible that HBpin may act as a hydride transfer reagent to provide short-lived zinc hydride and boryl species as intermediates during the formation of **4** with elimination of Zn , Cp^*H , and B_2pin_2 . We have previously reported somewhat unstable $\text{Zn}(\text{i})$ hydridoborate species $[(\text{TEEDA})\text{Zn}(\text{HBPh}_3)-\text{ZnCp}^*]$.¹⁶ The formation of zinc(ii) hydrides from HBpin was reported by Ingleson *et al.*²¹ However, the zinc(ii) hydride cation $[(\text{Me}_4\text{TACD})\text{ZnH}]^+$, previously isolated as $[(\text{Me}_4\text{TACD})\text{ZnH}][\text{HBPh}_3]^{16}$ is stable with respect to dehydrocoupling. Xu *et al.* reported that the dehydrocoupling of zinc(ii) hydride with a tridentate L_2X -type ligand forms the zinc(i)–zinc(i) bonded complex, but the reaction requires the presence of catalytic $[\text{Ni}(\text{CO})_2(\text{PPh}_3)_2]$ or stoichiometric $[\text{Pd}(\text{PPh}_3)_4]$.²² At this point, however, we cannot exclude other mechanistic pathways for the formation of **4**, including radical intermediates.^{22a,23}

In conclusion, we have prepared hypervalent zinc(i) complexes that contain the L_4 -type macrocycle Me_4TACD **1** and **4**. While the heteroleptic complex **1** can be accessed by protonolysis of dizincocene $\text{Cp}^*\text{Zn}-\text{ZnCp}^*$ using the conjugate acid of Me_4TACD , the homoleptic complex **4** was only obtained by the treatment of **1** with the hydride reagent HBpin in a somewhat complicated reaction. The reaction of **1** with activated hydrocarbons acetonitrile ($\text{pK}_a = 25$) and phenylacetylene ($\text{pK}_a = 29$) suggests that C–H bond cleavage by the dinuclear zinc(i)–zinc(i) complexes can occur by a polarized zinc(i)–zinc(i) bond, possibly

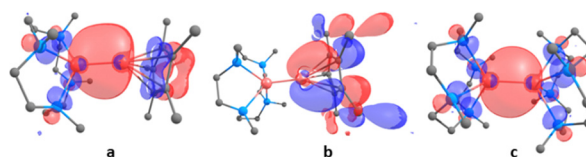


Fig. 3 (a) HOMO–2 for compound **1**. (b) HOMO for compound **1**. (c) HOMO for compound **4**.



in the presence of a Brønsted base. While C–H bond activation has been reported for d-block transition metals,²⁴ zinc(II) complexes appear to show similar reactivity with relevance to C–H bond functionalization.¹⁰

We thank Dr Louis J. Morris for helpful discussions.

Data availability

The data supporting this article have been included as part of the ESI.†

Conflicts of interest

There are no conflicts to declare.

Notes and references

- (a) I. Resa, E. Carmona, E. Gutierrez-Puebla and A. Monge, *Science*, 2004, **305**, 1136–1138; (b) A. Gorrirane, I. Resa, A. Rodriguez, E. Carmona, E. Alvarez, E. Gutierrez-Puebla, A. Monge, A. Galindo, D. del Rio and R. A. Andersen, *J. Am. Chem. Soc.*, 2006, **129**, 693–703.
- (a) M. L. H. Green and G. Parkin, *J. Chem. Educ.*, 2014, **91**, 807–816; (b) J. B. Jensen, *J. Chem. Educ.*, 2003, **80**, 952–961.
- Z. Zhu, M. Brynda, R. J. Wright, R. C. Fischer, W. A. Merrill, E. Rivard, R. Wolf, J. C. Fetting, M. M. Olmstead and P. P. Power, *J. Am. Chem. Soc.*, 2007, **129**, 10847–10857.
- Y. Wang, B. Quillian, P. Wei, H. Wang, X.-J. Yang, Y. Xie, R. B. King, P. V. R. Schleyer, H. F. Schaefer and G. H. Robinson, *J. Am. Chem. Soc.*, 2005, **127**, 11944–11945.
- K. Freitag, H. Banh, C. Ganesamoorthy, C. Gemel, R. W. Seidelb and R. A. Fischer, *Dalton Trans.*, 2013, **42**, 10540–10544.
- (a) S. Schulz, D. Schuchmann, I. Krossing, D. Himmel, D. Bläser and R. Boese, *Angew. Chem., Int. Ed.*, 2009, **48**, 5748–5751; (b) H. Banh, C. Gemel, R. W. Seidelb and R. A. Fischer, *Chem. Commun.*, 2015, **51**, 2170–2172.
- (a) M. L. H. Green and G. Parkin, *Dalton Trans.*, 2016, **45**, 18784–18795; (b) R. H. Crabtree, *Chem. Soc. Rev.*, 2017, **46**, 1720–1729.
- P. Mahawar, T. Rajeshkumar, T. P. Spaniol, L. Maron and J. Okuda, *Inorg. Chem.*, 2024, **63**, 8493–9501.
- J. T. Boronski, A. E. Crumpton, A. F. Roper and S. Aldridge, *Nat. Chem.*, 2024, **16**, 1295–1300.
- (a) I. L. Fedushkin, O. V. Eremenko, A. A. Skatova, A. V. Piskunov, G. K. Fukin, S. Y. Ketkov, E. Irran and H. Schumann, *Organometallics*, 2009, **28**, 3863–3868; (b) R. K. Sahoo, S. Rajput, A. G. Patro and S. Nembenna, *Dalton Trans.*, 2022, **51**, 16009–16016; (c) R. K. Sahoo, A. G. Patro, N. Sarkar and S. Nembenna, *ACS Omega*, 2023, **8**, 3452–3460; (d) T. Li, S. Schulz and P. W. Roesky, *Chem. Soc. Rev.*, 2012, **41**, 3759–3771.
- J. H. Coates, D. A. Hadi and S. F. Lincoln, *Aust. J. Chem.*, 1982, **35**, 903–909.
- (a) F.-G. Fontaine and V. Desrosiers, *Synthesis*, 2021, 4599–4613; (b) C. Jiang, O. Blacque and H. Berke, *Organometallics*, 2010, **29**, 125–133; (c) J. Guo, Ma Yan and D. W. Stephan, *Org. Chem. Front.*, 2024, **11**, 2375–2396.
- (a) J. Dyke, W. Levason, M. E. Light, D. Pugh, G. Reid, H. Bhakhoa, P. Ramasami and L. Rhyman, *Dalton Trans.*, 2015, **44**, 13853–13866; (b) H. Bhakhoa, L. Rhyman, E. P. Lee, D. K. W. Mok, P. Ramasami and J. M. Dyke, *Dalton Trans.*, 2017, **46**, 15301–15310; (c) P. Ghana and J. Okuda, *Bull. Jpn. Soc. Coord. Chem.*, 2021, **77**, 37–45.
- L. J. Morris, P. Ghana, T. Rajeshkumar, A. Carpentier, L. Maron and J. Okuda, *Angew. Chem., Int. Ed.*, 2022, **61**, e202114629.
- D. Schuhknecht, T. P. Spaniol, L. Maron and J. Okuda, *Angew. Chem., Int. Ed.*, 2020, **59**, 310–314.
- F. Ritter, L. J. Morris, K. N. McCabe, T. P. Spaniol, L. Maron and J. Okuda, *Inorg. Chem.*, 2021, **60**, 15583–15592.
- B. Li, K. Huse, C. Wölper and S. Schulz, *Chem. Commun.*, 2021, **57**, 13692–13695.
- (a) P. Jochmann and D. W. Stephan, *Angew. Chem., Int. Ed.*, 2013, **52**, 9831–9835; (b) P. Jochmann and D. W. Stephan, *Chem. – Eur. J.*, 2014, **20**, 8370–8378.
- (a) H. Brombacher and H. Vahrenkamp, *Inorg. Chem.*, 2004, **43**, 6054–6060; (b) P. Mahawar, T. Rajeshkumar, T. P. Spaniol, L. Maron and J. Okuda, *Chem. – Eur. J.*, 2024, **30**, e202401262.
- J. Prust, H. Hohmeister, A. Stasch, H. W. Roesky, J. Magull, E. Alexopoulos, I. Usón, H.-G. Schmidt and M. Noltemeyer, *Eur. J. Inorg. Chem.*, 2002, 2156–2162.
- M. Uzelac, K. Yuan, G. S. Nichol and M. L. J. Ingleson, *Dalton Trans.*, 2021, **50**, 14018–14026.
- (a) S. Jiang, Y. Cai, A. Carpentier, I. del Rosal, L. Maron and X. Xu, *Chem. Commun.*, 2021, **57**, 13696–13699; (b) M. Chen, S. Jiang, L. Maron and X. Xu, *Dalton Trans.*, 2019, **48**, 1931–1935; (c) S. Jiang, M. Chen and X. Xu, *Inorg. Chem.*, 2019, **58**, 13213–13220; (d) S. Xu, Q. Wang, T. Rajeshkumar, S. Jiang, L. Maron and X. Xu, *J. Am. Chem. Soc.*, 2024, **146**, 19590–19598.
- Y. L. Phang, J.-K. Jin, F.-L. Zhang and Y.-F. Wang, *Chem. Commun.*, 2024, **60**, 4275–4289.
- (a) T. Tanabe, M. E. Evans, W. W. Brennessel and W. D. Jones, *Organometallics*, 2011, **30**, 834–843; (b) Y.-H. Chang, K. Takeuchi, M. Wakioka and F. Ozawa, *Organometallics*, 2015, **34**, 1957–1962.

